Nonequilibrium Particle Morphology Development in Seeded Emulsion Polymerization. III. Effect of Initiator End Groups

Jeffrey M. Stubbs, Donald C. Sundberg

Polymer Research Group, Materials Science Program, University of New Hampshire, Durham, New Hampshire 03824

Received 28 June 2002; accepted 21 April 2003

ABSTRACT: In previous work (L. Karlsson et al., *Journal of Applied Polymer Science,* 2002, 2003, Vol. 90, pp. 905–915; J. M. Stubbs et al., *Colloids and Surfaces A: Physiochemical and Engineering Aspects,* 1999, Vol. 153, pp. 255–270) we have explained the development of composite particle morphologies produced by seeded emulsion polymerization in terms of the ability of second stage polymer radicals to diffuse into, or "penetrate," the seed particles. This has been quantified (Stubbs et al., ibid) by calculating so-called "fractional penetration" values for the second-stage radicals. In this article the effect of the second-stage initiator type, specifically nonionic vs ionic initiators, on particle morphology is investigated. The question to be answered is whether charged (ionic) end groups (from the initiator) on second stage polymer chains "anchor" to the particle surface, making it more likely to form core–shell morphologies. This is investigated by using a poly(methyl acrylate-co-methyl methacrylate) [P(MA-co-MMA)] seed latex and polymerizing styrene in the second stage in a semibatch manner using various feed rates of styrene. At each feed rate one reaction was conducted using potassium persulfate as the initiator, which produces charged end groups, and another using VA-086 initiator, which produces uncharged end groups. The morphologies of the resulting particles were then observed by transmission electron microscopy. It is shown that under some conditions ionic initiators do make it more likely to obtain core-shell morphologies, but that this effect is not dominant under most conditions. The resulting morphologies agree quite well with the predictions of the fractional penetration calculations. © 2003 Wiley Periodicals, Inc. J Appl Polym Sci 91: 1538–1551, 2004

Key words: latex; morphology; core-shell; nonequilibrium; initiator

INTRODUCTION

Structured (or composite) particles produced by seeded emulsion polymerization find applications as paints and coatings, adhesives, and impact modifiers.[1] There is great incentive to understand how to control the particle morphology because it is a large factor in determining the end use properties of the composite latex. Numerous formulation parameters are considered to be important in controlling particle morphology,[2] including surfactants,[3–5] initiators,[3,6] polymer type,[3,7] reaction temperature,[6,8,9–11] and crosslinking of the seed polymer.[12,13]

Depending on the conditions prevalent during the polymerization, the particle morphology will be determined either by thermodynamic or kinetic factors. Thermodynamic control of morphology is fairly well understood,[1,4,14–17] and is known to be driven by a minimization of the interfacial free energies of the system. The result of this minimization of interfacial energies is that in a majority of cases the more polar polymer forms at the outside of the particle. In this way the more hydrophilic polymer is in contact with the water phase. Numerous types of morphologies have been identified by researchers in the past few decades including core–shell (CS, the second-stage polymer forms a shell around the seed polymer), inverted core–shell (ICS, the seed polymer forms the shell), core–shell with internal occlusions (OCS), hemispheres, sandwich structures, and raspberry-like structures. It is noted here that there is confusion in the literature over the relationship between particle morphology and processing conditions. Often authors will refer to a "core-shell polymerization" in a way that assumes that the second-stage polymer will always form the shell, and is therefore referred to as the "shell polymer." Similarly, the seed polymer is often referred to as the "core polymer." It is important to note the error in this terminology as it stems from invalid assumption about how particle morphology is controlled. The fact that one polymer is fed in a second stage to a preformed seed latex does not necessarily mean that it will form a shell around the seed polymer, even though this is indeed sometimes the case.

More often than not, the conditions prevalent during a seeded emulsion polymerization are such that

Correspondence to: Donald C. Sundberg.

Contract grant sponsor: University of New Hampshire Latex Morphology Industrial Consortium (Mitsubishi Chemical, NeoResins, Atofina, and UCB Chemicals).

the thermodynamically favored particle morphology is not obtained. Instead, the morphology development may be controlled by kinetic considerations, producing a particle that is "frozen" in a nonequilibrium or thermodynamically unfavorable morphology. This type of situation often occurs when the T_g of the seed polymer is close to or above the reaction temperature, and the monomer is fed slowly during the second stage polymerization. This results in a very high viscosity within the seed particles during the polymerization making it difficult for the two polymer phases to rearrange into the equilibrium morphology. Previous investigations[18] have indicated that under these conditions the morphology development will be controlled by the very slow diffusion rates of polymer radicals within the particles, which may prevent the radicals from reaching the interior of the particles and thus confine the polymerization to an outer shell region, producing core–shell morphologies.

In the present article, the effect of initiator type on particle morphology was investigated under kinetically controlled conditions. The results are interpreted using a model we have developed[18] that aims to quantify the extent of penetration of the second stage polymer radicals into the seed particles during the polymerization. There is an ongoing debate in the emulsion polymerization literature over the extent to which radicals with ionically charged end groups are "anchored" to the particle surface by this charged end group. A charged end group on a polymer chain will result whenever an ionic initiator is used. This is an interesting topic in relation to the radical penetration concepts because it may affect the way in which radicals penetrate into particles and consequently have an effect on the particle morphology development.

It is safe to say that some of the polymer chain ends produced with an ionic initiator will indeed be anchored at the particle surface. This is because having charged end groups on the surface of the particles is commonly understood as being responsible for the colloidal stability of latices produced by surfactant free emulsion polymerization. In terms of stabilizing the particles against flocculation, these charged end groups behave similarly to surfactant molecules adsorbed on the particle surface. Various references are available which report on the relationship between the charge density on the particle surface and the latex stability.[19–21] Numerous other reports describe the measurement of charge densities on the particle surface,[20,22–25] thereby confirming the presence of charged groups on the surface. Numerous other researchers have either performed work under the assumption that charged radicals are surface anchored, or used surface anchoring to help explain experimental results.[19,20,26–30] However, it is also safe to say that not all charged end groups will be present on the surface. The fact that it is possible to produce inverted core–shell morphologies under certain conditions even when using a charged initiator in the second stage polymerization shows that it must be possible to "bury" these charged end groups. This was clearly shown in an earlier article[18] in which a poly(methyl acrylate) (PMA) seed latex was used and styrene was polymerized in the second stage and inverted core shell morphologies were obtained. In addition, Amalvy et al. investigated the spatial distribution of sodium and other elements in latex particles using electron spectroscopy imaging transmission electron microscopy (TEM) and found no evidence of an enriched concentration of the sulfate end groups at the particle surface.[31]

Another important point related to surface anchoring of charged end groups is to note that even when an ionic initiator is used, not all of the end groups on the polymer chains will be charged. This is because of the possibility that the initiator or end group may undergo a chemical reaction that will produce an end group that is a different chemical species entirely and may or may not be charged. For instance, one such reaction that is commonly known to occur with the sulfato radical produced from persulfate initiator is the hydrolysis reaction with water to produce a hydroxyl radical[32] (the solid bullet • symbol denotes a radical species).

$$\bullet\, SO_4^- + H_2O \rightarrow HSO_4^- + \bullet\, OH$$

This hydroxyl radical may then initiate polymerization in the water phase forming an hydroxyl end group on the polymer chain. Since this end group will not be charged, there is no reason to think that it would be anchored at the surface.

Palit et al.[32,33] studied the extent to which the hydrolysis of sulfate end groups occurs by using a dye partition test[34] to look at the fraction of polymer chains initiated by potassium persulfate, which had either sulfate or hydroxyl end groups. He found that hydroxyl end groups were always present to a fair extent. He also showed that the fraction of the total end groups that were hydroxyl was very dependent on the pH of the polymerizing medium. This fraction increased with decreasing pH, and could account for more than half of the total end groups when polymerized under very acidic conditions.

In another study, Tauer[21] used matrix assisted laser desorption ionization–time of flight (MALDI-TOF) mass spectrometry show that there were several possible species that could make up the end groups, including uncharged H and OH end groups, when using postassium persulfate (KPS) initiator. This information about the types of end groups that will result, even when using an ionic initiator, is very important

when considering the effect on particle morphology. It shows that even if charged radicals from ionic initiator do in fact anchor to the surface, this may not have an absolutely controlling effect on the particle morphology because many of the radicals will not be charged and will penetrate the particles more easily.

The goal of this article is to determine if charged end groups make it more likely to obtain core shell morphologies by preventing radicals from fully penetrating the seed particles. A series of seeded emulsion polymerizations have been performed, using both charged and uncharged initiators, in order to observe the effect on the particle morphology.

FRACTIONAL PENETRATION CALCULATIONS

We have developed a method that estimates the distance that an entering radical can penetrate into a seed particle.[18] The calculation takes into account the fact that as the radical grows, its diffusion coefficient drops sharply and thus the rate at which it diffuses into the particle continuously decreases.

The distance, Δx, that a radical chain end can move in a given time, Δt, is calculated using an approximate equation for the mean square distance moved by a diffusing species:

$$(\Delta x)^2 = (D_P \Delta t) \tag{1}$$

The diffusion coefficient for the radical, D_P, is the sum of both center of mass diffusion of the radical chain and movement of the active radical chain end through the addition of monomer units (known as reaction diffusion).[19] The center of mass diffusion coefficient, D_i^{com}, and reaction diffusion coefficient, D^{rd}, are given by

$$D^{\text{rd}} = (1/6) k_P C_P a^2 \tag{2}$$

$$D_i^{\text{com}} = D_{\text{mon}}(w_P)/i^2 \tag{3}$$

where $D_{\text{mon}}(w_P)$ is the diffusion coefficient for the monomer as a function of polymer weight fraction, w_P, C_P is the monomer concentration within the particles, i is the number of monomeric repeat units in the radical chain and a is the root-mean-square end-to-end distance per square root of the number of monomer units in a polymer chain, i.e. a is the mean distance moved, in a random flight sense, at each propagation step.[19] D_P is then computed from eq. (4):

$$D_P = D_i^{\text{com}} + D^{\text{rd}} \tag{4}$$

The dynamic simulation starts with an oligomeric radical with a chain length of z units at the surface of the particle (z is the critical degree of polymerization for entry of radicals into particles[19,35] and is equal to 2 for styrene monomer). The radical chain length, i, is increased by one unit for each time interval equal to $1/(k_P C_P)$, the average time between propagation steps. The diffusion coefficient is calculated from eqs. (2)–(4) and the mean squared distance moved, $(\Delta x)^2$, during each time step, Δt, from eq. (1). The total distance moved is determined simply by summing up the mean squared distances for all of the time steps from eq. (1) and then taking the square root. The total time that the simulation is carried out is equal to the average lifetime of a radical. One requirement of eq. (1) is that the diffusion coefficient must be constant over the time interval,[36] Δt. Therefore, the maximum time step allowable is equal $1/(k_p C_p)$ since each time the radical propagates, D_P will decrease.

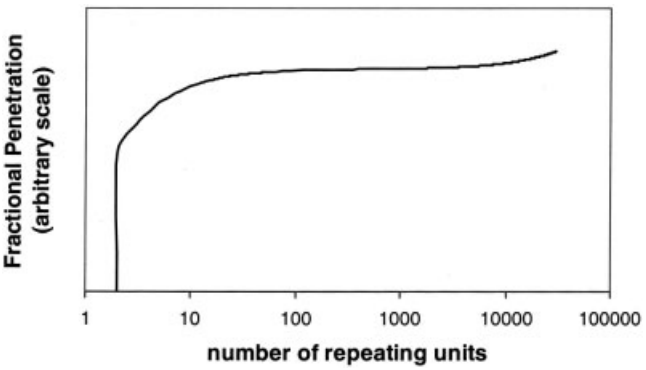

Figure 1 Typical fractional penetration of a radical into a seed particle.

The results of this simulation can be shown as graphs of the incremental fractional penetration (i.e., distance moved divided by particle radius) vs either time or chain length. Also, a value FP, the final fractional penetration, is defined as the total distance the radical can move during its entire lifetime divided by the particle radius. When FP is greater than or equal to 1, it is expected that the radicals will be able to penetrate completely into the seed particles and therefore morphologies deviating from core-shell will be possible.

A typical graph of fractional penetration versus the log of the chain length is shown in Figure 1. The important point to note is that the majority of the distance that the radical penetrates occurs while the radical is very short, less than about 10 units. This initial rapid penetration is a result of center of mass diffusion of the short radical. As the chain grows, center of mass diffusion can become negligible and the movement of the radical chain end becomes controlled by reaction diffusion. This is represented by the decreased slope of the later part of the curve that continues for the rest of the radical's lifetime.

In order to perform the fractional penetration calculations, it is necessary to estimate the average lifetime

of a radical. This has been calculated directly from the experimental results by using the pseudo-steady state assumption, which states that the rate of initiation of radicals is equal to the rate of termination of radicals. For an emulsion polymerization the rate of initiation is described more accurately by the rate of entry of radicals into particles. The equations for entry are available.[19] From this treatment the following equation for the average lifetime of a radical is developed:

$$\text{radical lifetime} = \frac{1}{k_t[R]} = \frac{V_{tp}[R]}{2fk_d[I]V_w} \quad (5)$$

where $[I]$ is the initiator concentration in the water phase, k_t is the apparent termination rate coefficient, V_w and V_{tp} are the volumes of water and particle phase in the reactor, respectively, $[R]$ is the radical concentration in the particle phase, and k_d is the dissociation rate coefficient of the intiator. The parameter f in eq. (5) is the entry efficiency for radicals into particles, which was calculated by the equations given by Gilbert.[19] This gives a value of f equal to 0.33. The radical concentration in the particles can be calculated directly from the experimental conversion vs time data, and all of the other terms are known from the recipe.

Three different types of FP calculations were performed in order to allow comparison between the experiments and to predict how large of an effect should be expected due to radical anchoring. The first type is the same as was described earlier and used in the previous publication.[18] This type assumes that the radicals are not anchored and can freely diffuse into particles after entry. It has been termed the unanchored fractional penetration and designated as FP_F, where the subscript F stands for free to penetrate. Values for FP_F have been calculated for all of the experiments. The second type of fractional penetration calculation assumes that the radicals are anchored at the particle surface and has been called the anchored fractional penetration, or FP_A. This has been calculated only for experiments that use KPS as the initiator. It is calculated simply by setting the center of mass diffusion coefficient, D_i^{com}, equal to zero. This is done because an anchored radical should only be able to move only by reaction diffusion.

The third type of fractional penetration is called the dead chain fractional penetration, or FP_D. This is a simple calculation since the length of a dead chain is not changing so D_i^{com} has a value that changes only as the monomer concentration may change, and for a dead chain $D^{rd} = 0$. This calculation simply estimates how far a dead chain of the average length can move during the duration of the experiment. This time scale is considered relevant because after this the latex is cooled and at room temperature the diffusion rates within the particles will decrease greatly (at room temperature the polymers used in the present experiments are in the glassy state). The average length of a chain is predicted roughly using the monomer concentrations and calculated radical lifetimes. However, in this case it is also necessary to consider chain transfer to monomer in order to predict the average length of a dead polymer chain given by

$$\frac{1}{\text{average\_dead\_length}} = \frac{1/(k_pC_{p,ca})}{\text{radical\_lifetime}} + \frac{k_{tr,m}}{k_p} \quad (6)$$

where $k_{tr,m}$ is the rate coefficient for chain transfer to monomer and the radical lifetime is given by eq. (5). For styrene at 70°C the value of $k_{tr,m}$ is equal to 2.9×10^{-2} L/mol/s.[37] FP_D can then be calculated directly from eq. (1) and dividing by the particle radius. This calculation uses Δt equal to the total time of the experiment and the diffusion coefficient calculated from eq. (3), with i calculated by eq. (6). This is an interesting calculation because it shows whether or not a polymer chain can diffuse further within a particle at a later time and cause a change in morphology. Extensions of this calculation can be done to estimate the anticipated change in morphology upon storage of the latex after production.

SIMILAR EXPERIMENTS FROM LITERATURE

A review of the literature revealed that some work along these lines has been done previously by Jönsson et al.[11] He performed polymerizations with a poly (methyl methacrylate) (PMMA) seed latex and styrene as the second-stage monomer and compared the effect of charged (KPS) vs uncharged [*t*-butyl hydroperoxide (t-BHP)] initiators on the resulting particle morphologies. The morphological results showed that core–shell morphologies resulted in all semicontinuous experiments regardless of whether KPS or t-BHP initiators were used. This suggested that, for these particular experiments, uncharged radicals were not able to penetrate the particles any easier than charged ones.

However, the penetration concepts described previously would suggest that these experiments have not actually succeeded in answering this question. This is because the experiments used a PMMA seed (T_g = 119°C) and performed experiments at a reaction temperature of 60°C. Therefore, at the low monomer concentrations typical of semicontinuous emulsion polymerization (less than 1 mol/L in the particle phase), the seed polymer was in the glassy state during the reaction. This results in very small monomer diffusion coefficients in the particles, which are estimated to be around 10^{-14} cm^2/s.[38] Representative fractional penetration calculations show that at these conditions very little penetration of the radicals is

TABLE I
Recipe and Conditions for the Controlled Copolymerization of MMA and MA to Produce the Seed Latex Used in All Second-Stage Polymerizations

Initial stage		Growth stage	
Experiment	jms3-19	Experiment	jms3-20
Water (g)	858.23	Latex from initial stage (g)	543.0
Sodium dodecyl sulfate (g)	0.4035	Water (g)	368.57
Potassium persulfate (g)	0.5046	Potassium persulfate (g)	0.3184
Sodium bicarbonate (g)	0.4825	Sodium bicarbonate (g)	0.2046
Initial MMA charge (g)	60.0	Initial MMA charge (g)	36.1
Initial MA charge (g)	90.1	Initial MA charge (g)	54
MMA addition after 21 min (g)	18.1	MMA addition after 21 min (g)	10.88
MMA addition after 37 min (g)	11.3	MMA addition after 37 min (g)	6.76
Temperature (°C)	70	Temperature (°C)	70
Final particle size (nm)	150	Final particle size (nm)	188
Final solid content (%)	17.35	Final solid content (%)	19.42

possible even for unanchored radicals, and the morphologies will be limited to core shell. This means that the question of whether the radicals are anchored or not is irrelevant in relation to morphology development under these experimental conditions.

In order to investigate the question of radical anchoring, it is necessary to perform the polymerizations using a seed latex for which full penetration of radicals is possible at faster monomer feed rates but somewhat restricted for slower monomer feed rates. In this case, if identical experiments at various monomer feed rates are performed using both charged and uncharged initiators, somewhere along the way a difference in the morphology produced by the two different initiators should be observed if surface anchoring does in fact affect the particle morphology. To determine the type of seed polymer that should be used, the work of Karlsson[8] and Ivarsson[9] was consulted. This work suggested that a seed latex consisting of a copolymer of PMA and PMMA with a T_g of about 55°C, and at a reaction temperature of 70°C, would be suitable for the purposes of the present work.

EXPERIMENTAL

Chemicals

Styrene, methyl acrylate, and methyl methacrylate monomers (Acros Organics, New Jersey) were passed through a column of alumina adsorption powder (80–200 mesh, Fisher Scientific, New Jersey) to remove inhibitors and stored at −10°C. Potassium persulfate, (analytical grade, Acros Organics) and VA-086 (2,2-Azobis[2-methyl-N-(2-hydroxyethyl) propionamide], Wako Chemicals, Inc., Osaka, Japan) were the inititators used and were used as received. Analytical grade sodium bicarbonate (EM Science, New Jersey) was the buffer. Sodium dodecyl sulfate (99%, Acros Organics) was used as received. Deionized water from a Corning Mega Pure™ D2 water purification system was used in all experiments.

Latex characterization

The monomer conversion of samples withdrawn from the reactor throughout the polymerization was measured gravimetrically. Particle sizes of the final latices and of intermediate samples were measured by quasi-elastic light scattering (QUELS) using a Coulter® Nanosizer™. The glass transition temperature of the seed latex was determined using a Perkin Elmer Pyris 1 Differential Scanning Calorimeter.

Transmission electron microscopy

Samples of the final latices were dried at room temperature to remove water, and then ground into a powder. A small amount of the powder was then embedded in EPON 812 epoxy (Fluka Chemical Corp.) and cured at 60°C for 8 h. Microtomed sections of approximately 90 nm thickness were observed in a Hitachi H600 transmission electron microscope. It was not necessary to stain the samples, as there is already adequate contrast between polystyrene and the p(MA-co-MMA) phases in the microscope.

Seed latex preparation

For the copolymerization of MA and MMA it was necessary to take steps to reduce the amount of compositional drift taking place. There is a tendency for compositional drift to occur in this system due to the reactivity ratios, $r_1 = 2.15$ and $r_2 = 0.4$ for MMA(1) and MA(2),[8,9] causing the MMA to be preferentially incorporated into the copolymer. This results in a copolymer with a range of temperatures spanning the glass transition, which is counterproductive since the reason for using a copolymer seed in these experi-

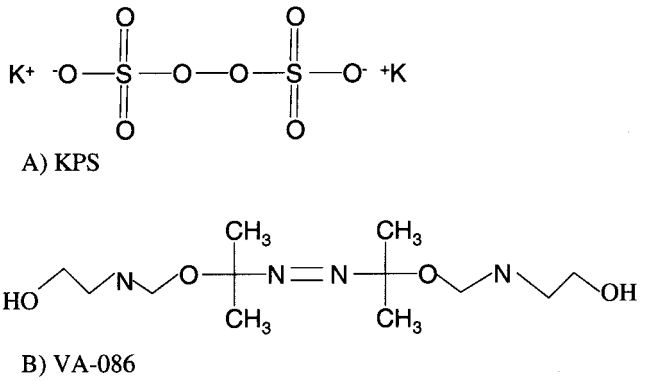

Figure 2 Molecular structures of the initiators used in the second-stage polymerizations.

ments is to allow control over the glass transition temperature. A monomer addition scheme was used in which a portion of the MMA was held back and added to the reactor in multiple steps at a later point during the reaction. This monomer addition scheme is specified in Table I, along with the recipe for the production of the seed latex. It was necessary to conduct the seed latex preparation in two separate stages to increase the size of the particles towards the desired 200 nm using a second growth stage.

The glass transition temperature of the dry seed copolymer produced was determined by differential scanning calorimetry (DSC) to be equal to 54°C. The final latex produced was repeatedly passed through a column of ionic exchange resins (Barnstead/Thermolyne) to remove residual initiator (the surfactant and buffer will also be removed in this case). This step was necessary to allow the initiator type and concentration to be carefully controlled during the second-stage polymerizations. After ion exchange the solid content of the latex had been reduced to 16.57%. All of the second stage polymerizations used this latex as the seed, except for one experiment (jms3–16). The latter experiment used a seed latex that was produced in an identical manner and resulted in the same particle size (188 nm) and a similar T_g of 52°C, but with a different solid content. The recipe for this experiment was adjusted to give the same starting solid content as the others.

Second-stage polymerizations

The second-stage polymerizations were conducted in a 250 mL glass reaction flask equipped with a water jacket and the temperature was regulated at 70°C under a nitrogen atmosphere. Stirring was performed using a magnetic stirrer at a rate fast enough to prevent the monomer from pooling as it was added to the reactor.

All ingredients except the monomer and initiator were added to the reactor, giving an initial solid content of 6%. Once the contents of the reactor reached 70°C, the initiator solution was added and the monomer and initiator (if necessary) feeds were started. The total amount of styrene added during the reaction was determined in order to give a stage ratio (mass of second stage monomer to mass of seed polymer) of 1:1. Experiments were conducted at various monomer feed rates, with the total styrene being fed over $\frac{1}{2}$, 1, 2, 4, and 8 h. For the polymerizations with the 1-h feed time, repeat experiments were performed to check reproducibility. For each monomer feed rate two experiments were performed, one using KPS as the initiator, and the other using VA-086. The molecular structures of both KPS and VA-086 are shown in Figure 2.

The initiator concentrations were calculated in order to give approximately the same rate of radical production for each initiator. The value of k_d at 70°C for KPS[19] (2.2×10^{-5} s^{-1}) is greater than that for VA-086 (3.83×10^{-6} s^{-1}).[39] Therefore, a higher molar concentration of VA-086 was required in those reactions.

When using KPS initiator, additional KPS was added continuously in the form of a 0.01 *M* aqueous solution fed at 0.6 mL/h to account for the KPS dissociating to form radicals and keep a constant KPS

TABLE II
Experimental Conditions for the Second-Stage Experiments with KPS as Initiator

Feed time (h)	$\frac{1}{2}$	1	1	2	4	8
Experiment	jms3-34	jms3-16	jms3-26	jms3-28	jms3-27	jms3-30
Seed latex (g)	72.4713	114.9978	72.4942	72.4012	72.4063	72.4526
DI water (g)	120.3378	77.5624	120.3255	120.3278	102.3133	120.3357
0.01*M* KPS solution (g)	7.6693	7.5945	7.6128	7.6287	7.6167	7.6510
$NaHCO_3$ (g)	0.0950	0.0942	0.0938	0.0947	0.0934	0.0965
SDS (g)	0.1109	0.1879	0.1131	0.1111	0.1116	0.1118
Total styrene fed (g)	12	12	12	12	12	12
Styrene feed rate (mL/h)	26.4	13.2	13.2	6.6	3.3	1.7
Total KPS solution fed (mL)	1.50	1.77	1.80	2.14	3.28	5.61
KPS feed rate (mL/h)	0.6	0.6	0.6	0.6	0.6	0.6
Temperature (°C)	70	70	70	70	70	70

TABLE III
Experimental Conditions for the Second-Stage Experiments with VA-086 as Initiator

Feed time (h)	$\frac{1}{2}$	1	1	2	4	8
Experiment	jms3-35	jms3-23	jms3-24	jms3-25	jms3-22	jms3-29
Seed latex (g)	72.4681	72.4686	72.4705	72.4745	72.4261	72.4081
DI water (g)	120.2880	120.2923	120.2923	120.3081	120.2865	120.2925
0.06*M* VA-086 solution (g)	7.3293	7.3197	7.3361	7.2973	7.3285	7.3090
$NaHCO_3$ (g)	0.0969	0.0983	0.0939	0.0974	0.0951	0.0941
SDS (g)	0.1124	0.1115	0.1118	0.1114	0.1106	0.1127
Total styrene fed (g)	12	12	12	12	12	12
Styrene feed rate (mL/h)	26.4	13.2	13.2	6.6	3.3	1.7
Temperature (°C)	70	70	70	70	70	70

concentration, and thus ensure a constant rate of radical production. This was not necessary when using VA-086 because its decomposition rate is slow enough so that the change in concentration over the course of the reaction is negligible. The experimental conditions for the experiments using KPS initiator are shown in Table II, and for those using VA-086 in Table III.

RESULTS AND DISCUSSION

The conversion of monomer to polymer and the monomer concentration within the particles are calculated easily by combining the solid content data obtained from gravimetric analysis of samples removed during the reaction with a mass balance calculation. A typical conversion profile for one representative experiment is shown in Figure 3. The most important point to take from this graph is that the reaction is close to steady state during the majority of the reaction. This is evident because the conversion line is essentially parallel to the monomer feed line. From the conversion vs time data it is straightforward to calculate the polymerization rate, radical concentrations within the particles and radical lifetimes throughout the various reactions. The kinetic data were used to calculate FP values for all of the experiments, which are then to be compared to the morphologies as observed by TEM. However, a slight adjustment of the experimental data (due to slight differences in the final monomer conversions for the different experiments) was first performed in order to provide more consistency and allow more meaningful comparisons to be made between the different experiments. This is discussed in more detail in the Appendix.

In order to calculate FP values for the experiments, two pieces of information are needed from the experimental results. These are (1) the monomer concentration, which determines how fast the radicals will propagate and also has a large effect on the diffusion coefficients; and (2) the radical lifetime, as this determines how long the FP simulation will be carried out. However, in order to calculate FP values to allow easy comparison between the different experiments, it is necessary to use single values for the monomer concentration and radical lifetime for each experiment. As discussed below, some approximations were necessary since the values of both of these parameters change somewhat during the course of the reactions.

The choice of the radical lifetime is relatively simple. This is because, as discussed earlier, the majority of the distance that the radicals penetrate occurs very soon after entry, while the radicals are very short, so

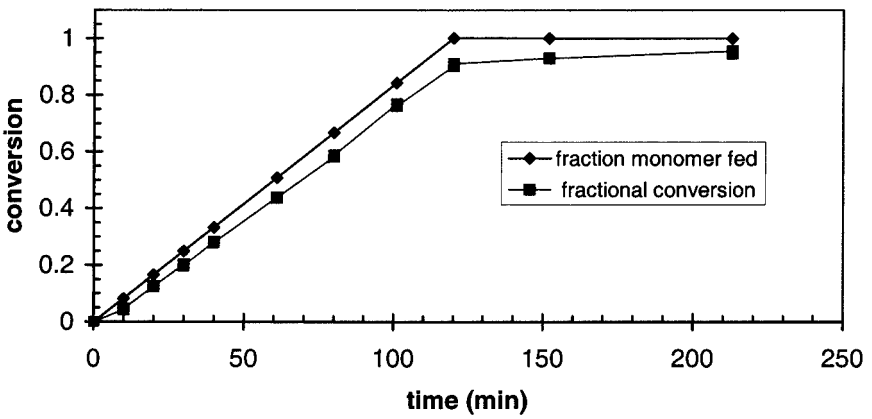

Figure 3 Typical conversion profile for a representative second-stage polymerization: styrene fed over 2 h with KPS initiator (jms3-28).

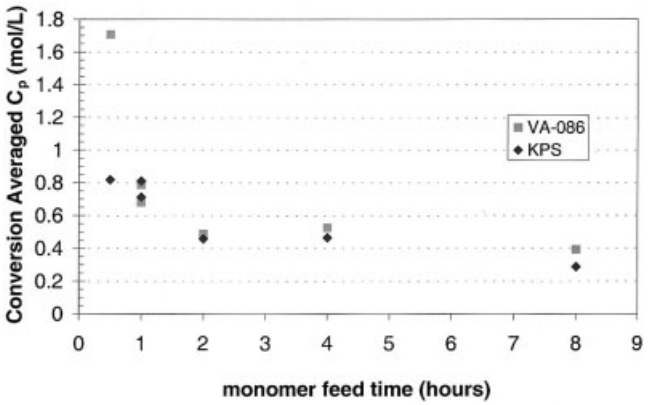

Figure 4 Conversion-averaged monomer concentration vs monomer feed time for all of the second-stage polymerizations.

small errors in the radical lifetimes have little effect on the FP calculations. The radical lifetime was taken as the average of the values calculated for the samples withdrawn after the system had reached a relatively steady state, and before the end of the monomer feed time. The choice of the proper value for the monomer concentration is more critical because this affects both the diffusion rates and propagation rates of radicals, and both of these have a significant effect on the FP calculation. The decision was made to use conversion-averaged monomer concentrations in the FP calculations. This value should reflect the conditions under which the majority of the second-stage polymer was formed, while at the same time not being blind to the regions of higher concentrations (as with faster monomer feed rates before the reactions reached steady state), since these regions would still have some effect on the final morphology. The conversion averaged monomer concentration is calculated according to

$$C_{p,\mathrm{ca}} = \frac{\int_0^{X_{\mathrm{fin}}} C_p(X)dX}{X_{\mathrm{fin}}} \tag{7}$$

where $C_{p,\mathrm{ca}}$ is the conversion averaged monomer concentration, $C_p(X)$ is the monomer concentration at a conversion of X, and X_{fin} is the final conversion level reached.

Figure 4 shows a plot of the conversion-averaged monomer concentrations versus the monomer feed time for all of the experiments. The first thing to note is that as the feed rate of monomer was increased (shorter feed times), the concentration of monomer within the particles during the reaction also increased, as would be expected. Therefore, at the faster monomer feed rates the diffusion rates of radicals within the particles will be faster. It is also clear that for the slower feed rates, when styrene was added over 2, 4, and 8 h, the monomer concentrations in the particles did not vary greatly. Therefore, for these polymerizations the diffusion rates of radicals will also be very similar.

The most important point to note from Figure 4 is that at a given feed rate, the monomer concentrations are almost always the same whether KPS or VA-086 was used as the initiator. This is a very important point because it suggests that, for a given monomer feed rate, the diffusion rates of radicals within the particles are the same regardless of which initiator was used (except for possible differences caused by anchoring at the particle surface).

It is also clear from Figure 4 that in one case, for the $\frac{1}{2}$-hour feed time, the monomer concentrations were not the same for the experiments with the two different initiators. This was the only case in which this was experienced. Here, the concentration for the polymerization using VA-086 is much greater than for KPS. The differences between these two experiments are clearly visible when comparing the conversion vs time results (not shown here for the sake of brevity). In all experiments except for the one with a $\frac{1}{2}$-h monomer feed time and VA-086 initiator, the conversion vs time profile was both close to and relatively parallel to the monomer addition vs time profile. In other words, the rate at which monomer was converted to polymer was equal to the rate at which monomer was being fed. However, in the experiment with the $\frac{1}{2}$ h feed time and VA-086 initiator, the conversion rate was slower than the monomer addition rate. This resulted in accumulation of monomer in the reactor, and is responsible for the higher monomer concentration observed in Figure 4 for this particular experiment.

In addition to the monomer concentrations and radical lifetimes, which are available from the experimental conversion data, values for k_p, the particle radius, and the diffusion coefficient for monomer are also required in order to calculate FP values. The value of k_p for styrene at 70°C is equal to 480 L/mol/s.[19] Since the particles grow during the second-stage polymerization from the seed particle radius of approximately 95 nm to a final radius of about 125 nm, an average radius of 110 nm was used in the FP calculations (the radius is only used to compare to the estimated distance that the radical diffuses, the ratio of the two is the FP value, as described earlier). Finally, the diffusion coefficients for monomer as a function of polymer weight fraction in the copolymer seed having a T_g of 54°C and at a reaction temperature of 70°C was estimated by a method described in a separate article.[38] These diffusion coefficients are shown graphically in Figure 5. One should note that the decrease in the monomer diffusion coefficients at high polymer weight fraction has the possibility of affecting the

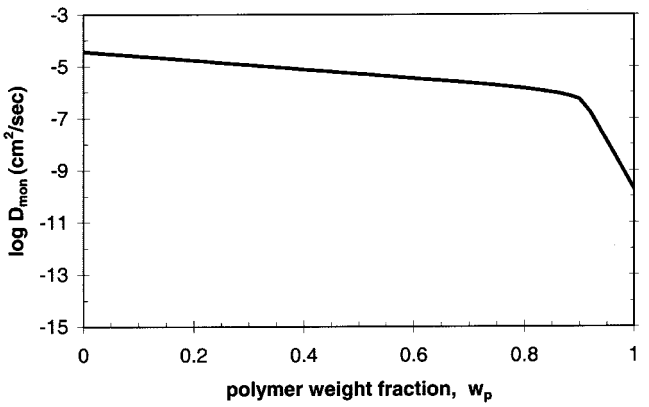

Figure 5 Estimated diffusion coefficients at 70°C for monomer in the P(MA-co-MMA) seed polymer (T_g = 54°C).

frequency of the propagation reactions, due to the fact that propagation can become diffusion controlled at high conversion. This would affect the penetration calculations, as it would affect the reaction diffusion coefficient, D^{rd}, as given by eq. (2). However, this effect does not occur in the present systems because the decrease in Dmon is not enough to cause a decrease in k_p, as calculated from applicable models.[19]

Some interesting points can be drawn by inspecting Figure 5 along with consideration of the magnitudes of the monomer concentrations for the experiments as shown in Figure 4. These monomer concentrations correspond to polymer weight fractions greater than 0.9, and are typical of semicontinuous polymerizations with slow monomer feed rates. These high polymer weight fractions also correspond to the same region where the diffusion coefficients start to decrease rapidly in Figure 5. Therefore, it is no surprise that it was under these same conditions of seed polymer T_g and reaction temperature that Karlsson et al.[8] found that they were able to change the morphological results by changing the monomer feed rate, as discussed previously. This is because a change in the monomer feed rate will cause a change in the monomer concentration, which for these reaction conditions will cause a significant change in the diffusion rates of the entering radicals.

FRACTIONAL PENETRATION PREDICTIONS AND PARTICLE MORPHOLOGIES

The final values for all three types of fractional penetration calculations for all of the various experiments are shown in Table IV, along with characteristic values that were used in these calculations as described in the previous section. One may note that the radical lifetimes in Table IV are rather large. This, along with high radical concentrations (number of radicals per particle), is common in semibatch emulsion polymerizations that sustain high instantaneous monomer conversion levels throughout the reaction. It may seem that these long lifetimes would have an impact on the fractional penetration calculations. However, as discussed previously in relation to Figure 1, the radical lifetime does not have a significant impact on the level of radical penetration because most of the penetration occurs early in the life of the radical while it is still a relatively short chain.

TEM micrographs showing the resulting particle morphologies are displayed in Figures 6–9 (pictures are of microtomed sections). The darker phase is polystyrene and the lighter phase is P(MA-co-MMA).

There are a few things that should be kept in mind when considering the various fractional penetration values and what they mean about the expected morphologies. The first is the fact that not all of the end groups formed by KPS initiator will be charged, as mentioned earlier. The penetration depth for this un-

TABLE IV
Fractional Penetration Values and Values of Quantities Used in the Calculations for All of the Various Experiments

Monomer feed time (h)	Initiator type	Experiment	$C_{p,ca}$ (mol/L)	Ave. radical lifetime (s)	$D_{mon}(w_p)$ (cm^2/s)	FP_F	FP_A	FP_D
$\frac{1}{2}$	KPS	jms3-34	0.818	166	1.12E-7	1.36	0.57	0.11
$\frac{1}{2}$	VA-086	jms3-35	1.705	34	3.55E-7	1.57	—	0.24
1	KPS	jms3-16	0.713	88	5.69E-8	1.02	0.39	.011
1	KPS	jms3-26	0.810	78	1.13E-7	1.30	0.39	0.15
1	VA-086	jms3-23	0.679	108	4.05E-8	0.93	—	0.08
1	VA-086	jms3-24	0.788	93	9.48E-8	1.23	—	0.13
2	KPS	jms3-28	0.458	61	6.76E-9	0.48	0.26	0.06
2	VA-086	jms3-25	0.487	43	9.51E-9	0.52	—	0.08
4	KPS	jms3-27	0.465	31	7.36E-9	0.46	0.18	0.11
4	VA-086	jms3-22	0.526	29	1.34E-8	0.59	—	0.15
8	KPS	jms3-30	0.287	21	1.73E-9	0.28	0.12	0.14
8	VA-086	jms3-29	0.392	18	4.42E-9	0.38	—	0.20

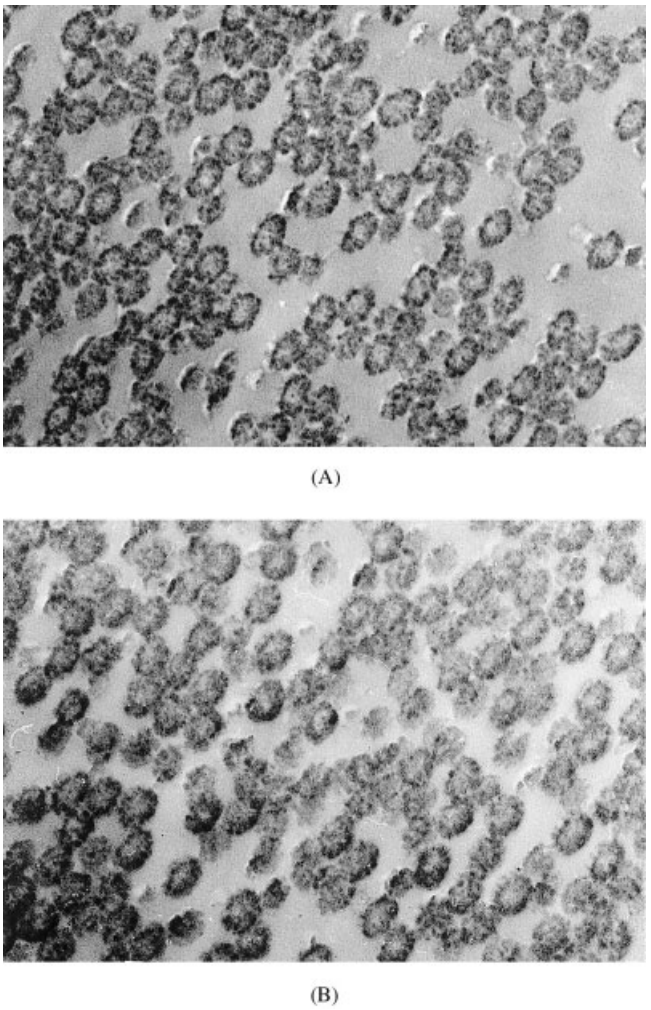

Figure 6 TEM photos of microtomed sections of latex particles for experiments with a 2-h monomer feed time. (A) KPS initiator (jms3-28); (B) VA-086 initiator (jms3-25). Reprinted with permission.[41]

charged fraction of radicals formed from KPS will be better predicted by the unanchored fractional penetration than by the anchored value. The second point is that it is known that under some conditions it is possible to bury charged end groups, as discussed earlier in the introduction section. It is not known at exactly what point these charges become buried. It may be that the new polymer being formed within the particle "buries" the end groups on previously formed polymer. It is also possible that charged radicals are anchored while they are relatively short, but as they become longer chains they may be able to pull the charged end group into the particle. This possibility is why the dead chain fractional penetration calculation is interesting, as it lends insight into the question of whether these longer chains would then be able to diffuse to the center of particles to form internal occlusions of second stage polymer. Inspection of the FP_D values in Table IV would suggest that in the present experiments the answer is no. The values are all around 0.1–0.2, so a dead chain would only be able to diffuse 10–20% of the particle radius during the entire duration of the experiment. Therefore, internal occlusions that may be seen in these experiments cannot have been formed by further diffusion of dead polymer causing rearrangement of the particle morphology during the experiment.

The last point that should be kept in mind is the possibility of chain transfer to monomer and its effect on radical penetration. When chain transfer occurs, it will result in a mobile monomeric free radical that can diffuse very quickly until it adds a few monomer units by propagation. Therefore even in cases where radicals are not able to reach the center of the particles, either due to anchoring or slow diffusion rates, the occurrence of transfer to monomer may allow radicals to reach the particle center. Keeping these above points in mind, one can get a feel for the effect that

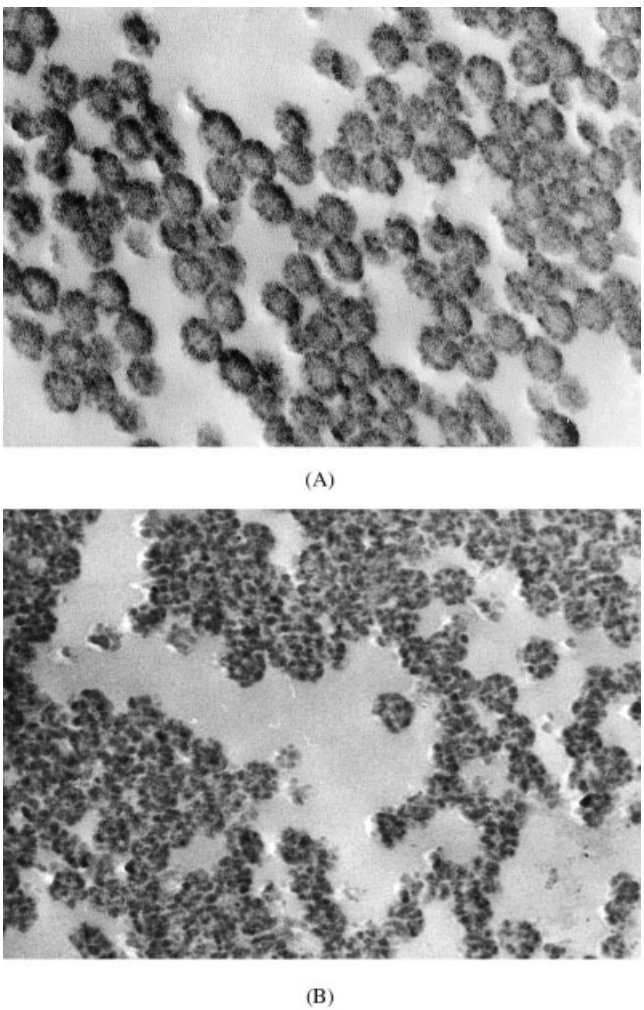

Figure 7 TEM photos of microtomed sections of latex particles for experiments with a 1-h monomer feed time. (A) KPS initiator (jms3-16); (B) VA-086 initiator (jms3-23). Reprinted with permission.[41]

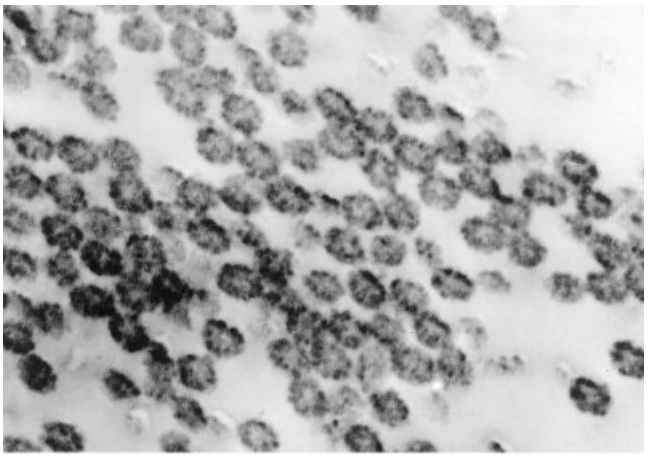

(A)

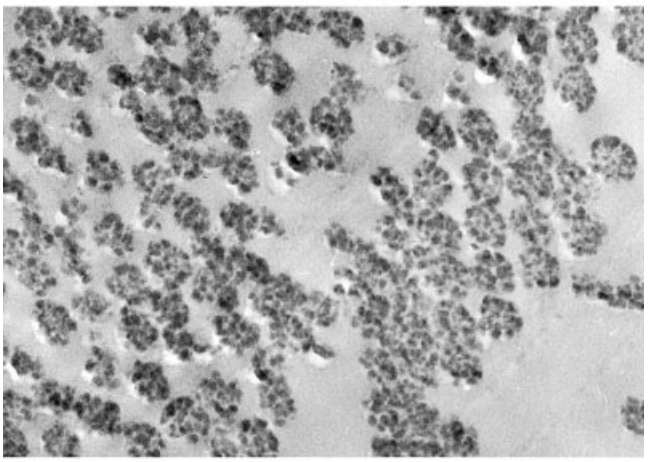

(B)

Figure 8 TEM photos of microtomed sections of latex particles for repeated experiments with a 1-h monomer feed time. (A) KPS initiator, (jms3-26); (B) VA-086 initiator (jms3-24).

should be expected in the present experiments if charge anchoring does affect morphology development by inspecting the values for the anchored and unanchored fractional penetrations. Table IV shows that for the 2-, 4- and 8-h feed times the values of FP_F are in the range of 0.5. For these same feed rates in the KPS experiments the values of FP_A are closer to 0.2. The FP_F values suggest that even if radicals are not anchored they will still not be able to diffuse all the way to the particle center. Therefore, in these experiments morphologies exhibiting a shell of polystyrene should be expected for either initiator. If anchoring is a factor, it may result in a more compact shell for the KPS reactions since the FP_A values are smaller. However, this would only be a slight difference in the observed morphologies and may be difficult to observe clearly. The fact that a fraction of the KPS derived radicals are uncharged will make the morphologies from the two different initiators even more similar, and more difficult to clearly observe differences in the TEM.

Figure 6(a,b) shows the morphology results for both the KPS and VA-086 polymerizations with a 2-h monomer feed time. In this case it is clear that the resulting morphology in both cases consists of a shell of polystyrene around the seed polymer, but also has many occlusions of polystyrene within the seed polymer core. In these pictures there is no obvious difference between the morphologies obtained with either initiator. Both these "occluded/core-shell" morphologies and the similarity between the morphologies for the different initiators agree with the predictions of the fractional penetration calculations for this monomer feed rate. The TEM photos for the experiments

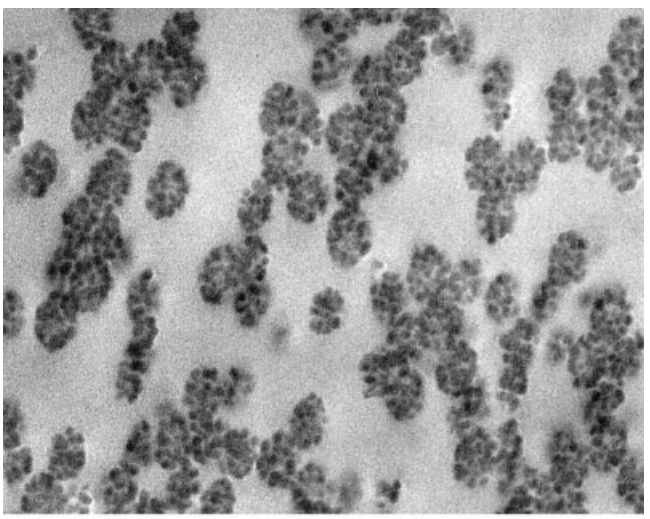

(A)

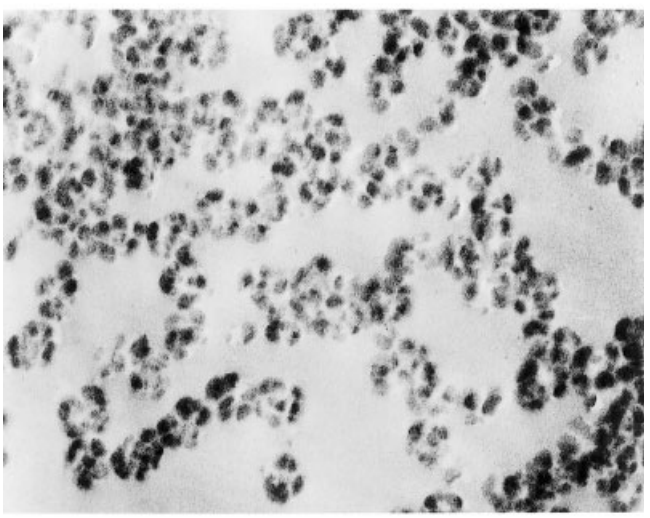

(B)

Figure 9 TEM photos of microtomed sections of latex particles for experiments with a $\frac{1}{2}$-h monomer feed time. (A) KPS initiator (jms3-34); (B) VA-086 initiator (jms3-35). Reprinted with permission.[41]

with the 4 and 8 hour feed times all showed the same occluded/core–shell morphologies as for the 2-h feed time in Figure 6, so they have not been included for the sake of brevity. There was still no observable difference in the morphologies obtained for the different initiators. Again, these results agree with the fractional penetration predictions. The identical morphologies for these three different monomer feed rates are predicted by the similarity in their fractional penetration values. This insensitivity to monomer feed rate over this range is due to the fact that the monomer concentrations within the particles for these experiments are all about the same, as is seen in Figure 4.

The relatively large amount of internal occlusions at the center of the particles in each case is also not surprising, even though the fractional penetrations predictions show that even unanchored radicals should only be able to penetrate about 50% of the radius. This may be because some amount of chain transfer to monomer will occur. Along these lines, we are currently conducting experiments to determine the effect of chain transfer agent on particle morphologies, and this will be reported in a subsequent paper.

The FP_F and FP_A values suggest that the more interesting experiments for investigating the effect of initiator end groups on particle morphology are those with the faster monomer feed rates. For the experiments with a 1-h feed time the FP_F values are in the range of 0.93–1.3 and for the $\frac{1}{2}$ hour feed time are closer to 1.5. This suggests that if radicals are not anchored, they should be able to diffuse to the center of the particles and the resulting particle morphologies should not have polystyrene shells. However, the FP_A values for the KPS experiments at these feed times are much less than 1.0 and suggest that anchoring of radicals would result in morphologies with polystyrene shells.

The morphology results for the reactions with a 1-h feed time are shown in Figure 7(a,b). Here, the experiment with the KPS initiator shows a similar occluded core–shell morphology as observed for the experiments with slower feed rates. However, for the experiment with the VA-086 initiator there is no shell of polystyrene around the particles. Instead, the morphology from this experiment is simply an occluded type with domains of polystyrene located uniformly throughout the particles. This clearly shows that the uncharged radicals from the VA-086 initiator were able to penetrate into the seed particles more easily than the charged radicals from the KPS initiator. The monomer concentrations are very close for the two experiments and result in very similar diffusion rates for the incoming radicals, giving rise to very similar predictions for the unanchored fractional penetration. Therefore, the difference in the observed morphology is most likely due to at least partial anchoring of the sulfate end group from the KPs at the particle surface. This prevents full penetration, as indicated by the smaller values calculated for the FP_A in the KPS experiment. The morphology results shown in Figure 8(a,b) are for repeat experiments at the 1-h feed time for either initiator. Again, the experiment with KPS showed a polystyrene shell on the particles while the experiment with VA-086, showing that this result is in fact real and reproducible.

The morphology results for the experiments with the fastest feed rate, when the styrene was fed over $\frac{1}{2}$ hour, are shown in Figure 9(a,b). In this figure it is clear that neither reaction resulted in a morphology with a shell of polystyrene and in both cases strictly occluded morphologies were obtained. This shows that anchoring of radicals alone cannot cause core–shell morphologies to be obtained in all cases when KPS is used as initiator in the second stage. It was shown by Karlsson[8] that for the same conditions of seed polymer T_g and reaction temperature and with KPS initiator, when the second-stage reaction was run under batch conditions an occluded morphology was obtained. This is partly because in a batch reaction the monomer concentration in the particles is high, therefore the internal particle viscosity is lower and the diffusion of radicals is faster. This same point was also shown by previous experiments a low T_g PMA seed[18] (thus giving a lower internal particle viscosity), which produced an inverted core–shell morphology. In the present case, when the styrene was fed at a fast rate such as with the 1/2 hour feed time, the conditions start to approach the batch case. Therefore, it is not surprising that an occluded morphology resulted even for KPS.

However, this result is not entirely predicted by the fractional penetration calculations. In the KPS reaction with the $\frac{1}{2}$ hour feed time the monomer concentration is only slightly greater than in the KPS reactions with a 1-h feed time, and the calculated FP values are also only slightly greater, but the resulting morphologies were much different. It is likely that this apparent similarity in the monomer concentrations is due to experimental error and that the actual monomer concentration in the $\frac{1}{2}$ hour experiment is actually greater than in the 1-h experiments. Common sense would say that this should be the case, since faster monomer feed rates usually result in higher monomer concentrations. Nevertheless, it is clear that at this faster monomer feed rate the condition was reached where even the radical chains with charged end groups were able to move inside the seed particles.

Another point that is clear from the morphology results for the $\frac{1}{2}$-hour experiments is that the size of the polystyrene domains in the experiment with VA-086 are much larger than those for the KPS experiment. This is surely due to the fact that the monomer concentration in the KPS experiment was significantly less than in the experiment with VA-086, as shown in

Figure 4 and discussed previously. This higher monomer concentration means that in the experiment with VA-086 the dead polymer chains will be able to diffuse more easily than in the KPS experiment. Diffusion of the polymer chains will allow more of the separate polystyrene domains to come together, resulting in increased consolidation of the phases and larger polystyrene domains. The driving force for this consolidation is a lowering of the total interfacial free energy of the system.

The existence of the many separate polystyrene domains in all of the observed morphologies means that the particles have not reached the equilibrium morphology. Therefore, the morphology is still being controlled by kinetic factors in these systems. This was the case even when full penetration is predicted and is not surprising. The fact that the radicals are able to penetrate the seed particles simply means that the morphology will not be restricted to core–shell. It does not mean that the equilibrium inverted core–shell morphology will be achieved. The penetration of polystyrene in this case occurs because when the short radicals enter the seed particles from the water phase, the diffusion rates within the particles are fast enough to allow them to reach the particle center before they get too long and their diffusion rate slows down. However, in order for full phase consolidation to occur, even the long radicals and dead polymer chains must be able to diffuse fast enough to allow the separate polystyrene domains to come together and consolidate the separate polymer phases.

CONCLUSIONS

It is clear from the experiments reported here that chain anchoring will only be an important mechanism in morphology control under some reaction conditions. As our calculations have shown, there are intermediate polymer radical diffusion rates that can highlight the difference between charged and uncharged initiators. Diffusion rates that are either much faster or much slower lead to the same morphological results for either initiator. Given that there are several other parameters (e.g., monomer feed rate, seed polymer T_g, reaction temperature, initiator concentration) which have more direct control on the polymer radical diffusivity within the particle, we conclude that chain anchoring due to initiator end groups alone is seldom a major factor in controlling morphology. Even when it appears that chain anchoring can be important, we are reminded that some sulfate radicals experience hydrolysis reactions, yielding some uncharged end groups. It is also clear that some sulfate end groups must become buried during the reaction (given the results of batch polymerizations) and also that chain transfer is significant in many processes, particularly those commercial recipes with added chain transfer agent. These events lead to significant penetration of polymer radicals within the particle and more often than not produce structures that contain a significant number of occlusions, even when an apparent shell is observed.

APPENDIX

This discussion relates to slight adjustments that were made to the experimental data before using it in the fractional penetration calculations. It was noticed that the final calculated conversion levels in the various experiments were not always the same. Instead, they varied between about 93 and 97%, with an average value for all of the experiments of 95.1%. It is well known that the limiting conversion of monomer to polymer is reached when the concentration of monomer in the polymer is such that the mixture is near the glass transition.[40] It should be expected that for all of the experiments discussed here the limiting conversion should be reached at the same monomer concentration in each experiment. This is simply because the same polymer is being produced in each reaction and the reaction temperature is always 70°C. Therefore, the observed variation in the final conversions for the various experiments is likely caused by experimental error instead of actual variations in the monomer concentrations at the end of the reaction.

It is important to note that even small experimental errors in the measured solid contents will cause significant change in the calculated values for monomer concentrations and rates. This is mostly due to the relatively low solid content and high instantaneous conversions prevalent during the experiments, so that the amount of monomer in the total latex at any time is only about 1%. This tends to make comparison between the different experiments more difficult. This is a problem because the major goal here is to compare differences in the morphology predictions and actual morphologies, in part due to the different monomer concentrations in the particles for experiments with different monomer feed rates causing faster or slower diffusion rates.

The following approach was adopted to overcome this problem. In the mass balance calculations, the total amount of water in each of the reactions was adjusted slightly in order to make the final conversion for each of the reactions equal to the average value of 95.1%. In all of the experiments, the adjustment of the total amount of water in the mass balance that was required to adjust the final conversion was no greater than 2.2 g, which corresponds to only about 1% of the total amount of water in the reactor. In most cases the adjustment was actually much less than this. Therefore, it is felt that this adjustment is not unreasonable and it allowed for a much more consistent comparison of the monomer concentrations calculated for the different experiments. For the

graphs in Figure 3 this adjustment of the final conversion have already been made.

References

1. Winzor, C. L.; Sundberg, D. C. Polymer 1992, 33, 3797–3810.
2. Dimonie, V.; Daniels, E.; Shaffer, O.; El-Aasser, M. In Emulsion Polymerization and Emulsion Polymers; Lovell, P. A., El-Aasser, M. S., Eds.; John Wiley & Sons Ltd.: Londons, 1997, pp 293–326.
3. Chen, Y.; Dimonie, V.; El-AAsser, M. Macromolecules 1991, 24, 3779.
4. Sundberg, D.; Cassasa, A.; Pantazopoulos, J.; Muscato, M.; Kronberg, B.; Berg, J. J Appl Polym Sci 1990, 41, 1425.
5. Yan, C.; Xu, Z.; Cheng, S.; Feng, L. J Appl Polym Sci 1998, 68, 969–975.
6. Lee, S.; Rudin, A. J Polym Sci, Part A: Polym Chem 1992, 30, 2211.
7. Sundberg, E.; Sundberg, D. J Appl Polym Sci 1993, 47, 1277.
8. Karlsson, L.; Karlsson, O. J.; Sundberg, D. C. J Appl Polym Sci 2003, 90, 905–915.
9. Ivarsson, L.; Karlsson, O.; Sundberg, D. Macromolecular Symposia 2000, 151, 407–412.
10. Jönsson, J.-E. L.; Hassander, H.; Jansson, L. H.; Törnell, B. Macromolecules 1991, 24, 126–131.
11. Jönsson, J.-E.; Hassander, H.; Törnell, B. Macromolecules 1994, 27, 1932–1937.
12. Durant, Y.; Sundberg, E.; Sundberg, D. Macromolecules 1996, 29, 8466.
13. Durant, Y.; Sundberg, E.; Sundberg, D. Macromolecules 1997, 30, 1028.
14. Berg, J.; Sundberg, D.; Kronberg, B. Polym Mater Sci Eng 1986, 54, 367.
15. Berg, J.; Sundberg, D.; Kronberg, B. J Microencapsulation 1989, 6, 327.
16. Durant, Y.; Sundberg, D. J Appl Polym Sci 1995, 58, 1607–1618.
17. Waters, J. Colloids and Surfaces A: Physiochemical and Engineering Aspects 1994, 83, 167.
18. Stubbs, J. M.; Karlsson, O. K.; Sundberg, E. J.; Durant, Y. G.; Jönsson, J. E.; Sundberg, D. C. Colloids and Surfaces A: Physiochemical and Engineering Aspects 1999, 153, 255–270.
19. Gilbert, R. G. Emulsion Polymerization: A Mechanistic Approach; Academic Press: London, 1995; pp 28, 31, 37, 71, 93.
20. Fitch, R. Polymer Colloids: A Comprehensive Introduction; Academic Press: San Diego, 1997.
21. Tauer, K.; Deckwer, R. Acta Polym 1998, 49, 411–4116.
22. Verwey, E.; Kruyt, H. Z Physik Chem 1933, A167, 149.
23. Stubbs, J. M.; Durant, Y. G.; Sundberg, D. C. Langmuir 1999, 15, 3250–3255.
24. Stone-Masui, J.; Stone, W. E. E. In Polymer Colloids II; Fitch, B., Ed., Plenum Press: New York, 1980, 331.
25. Fitch, R.; Su, L.; Tsaur, S. In Scientific Methods for the Study of Polymer Colloids and Their Applications, Vol. 303; Candau, F., Ottewil, R. H., Eds.; NATO ASI Series, Series C, Kluwer: Dordrecht, Netherlands, 1990; p 373.
26. Kukulj, D.; Gilbert, R. G. In Polymeric Dispersions: Principles and Applications; Vol. 335; Asua, J. M., Ed.; NATO ASI Series, Series E; Kluwer Academic Publishers: Dordrecht, 1997; pp 97–107.
27. Mills, M. F.; Gilbert, R. G.; Napper, D. H. Macromolecules 1990, 23, 4247–4257.
28. Chern, C.; Poehlein, G. J Polym Sci, Part A: Polym Chem 1987, 25, 617.
29. Croxtoń, C.; Mills, M.; Gilbert, R.; Napper, D. Macromolecules 1993, 26, 3563–3571.
30. Maxwell, I. A.; Kurja, J.; Van Doremaele, G. H.; German, A. L.; Morrison, B. R. Makromol Chem 1992, 193, 2049–2063.
31. Amalvy, J.; Asua, J.; Leite, C.; Galembeck, F. Polymer 2001, 42, 2479–2489.
32. Ghosh, P.; Chadha, S. C.; Mukherjee, A. R.; Palit, S. R. J Polym Sci, Part A 1964, 2, 4433–4440.
33. Ghosh, P.; Chadha, S. C.; Palit, S. R. J Polym Sci, Part A 1964, 2, 4441–4451.
34. Palit, S. R. Makromol Chem 1959, 36, 89.
35. Maxwell, I.; Morrison, B.; Napper, D.; Gilbert, R. Macromolecules 1991, 24, 1629–1640.
36. de Gennes, P. Scaling Concepts in Polymer Physics; Cornell University Press: Ithaca, NY, 1979.
37. Brandrup, J.; Immergut, E. H.; Grulke, E. A., Eds. Polymer Handbook, 4th ed.; John Wiley Sons: New York, 1999; p 102.
38. Karlsson, O.; Stubbs, J.; Karlsson, L.; Sundberg, D. Polymer 2001, 42, 4915–4923.
39. VA-086 Technical Information, Waco Chemicals USA, Inc., 1998.
40. Sundberg, D.; James, D. J Polym Sci, Polym Chem Ed 1978, 16, 523–529.
41. Sundberg, D. C.; Stubbs, J. M. J Coat Tech 2003, 75, 59–67.